Context-Aware Cognitive SIMO Transceiver for Increased LTE-Downlink Link-Level Throughput

Imen Mrissa, Faouzi Bellili, Sofiène Affes, and Alex Stephenne

INRS-EMT, 800 De La Gauchetiere W., Suite 6900, Montreal (Quebec), H5A 1K6, CANADA

Email: {mrissa,bellili,affes,stephenne}@emt.inrs.ca

Abstract—Coherent detection requires accurate channel estimation to provide the high data rates promised by the LTE standard. However, for high-speed wireless data transmission services, channel estimation becomes a challenging task when the pilot insertion rate becomes insufficient to allow proper tracking of the channel variation. In this paper, we design a new single-input multiple-output (SIMO) context-aware cognitive transceiver (CTR) that is able to switch to the best performing modem (modulation-demodulation) in terms of link-level throughput. For that purpose, on the top of conventional adaptive modulation and coding, we allow the context-aware CTR to make best selection among three different pilot-utilization modes: Conventional Data-Aided (DA) or pilot-assisted, Non-Data-Aided (NDA) or blind and Non-Data-Aided with pilot (NDA w. pilot) which is a newly proposed hybrid version between the DA and NDA modes. We also enable the CTR to make best selection between two different channel identification schemes: conventional Least Squares (LS)-type and newly developed Maximum Likelihood (ML) estimators. Depending on whether pilot symbols are used or not, we further enable the CTR to make best selection among two data detection modes: coherent or differential. Owing to extensive and exhaustive LTE-downlink link-level simulations, we are able to draw out the decision rules of the new CTR that identify the best combination triplet of pilot-use, channel-identification, and data-detection modes. The latter is able to achieve the best link-level performance against any given operating conditions in terms of channel type, mobile speed, SNR, and Channel Quality Indicator (CQI). Significant link-level throughput gains of the new proposed CTR against the conventional one (i.e., pilot-assisted LS-type channel estimation with coherent detection) can be achieved in most operating conditions and could reach as much as 700% at low SNR and high mobility!

I. INTRODUCTION

One of the strongest driving forces for wireless technology evolution today is 4G (4th Generation), also known as LTE-Advanced (Long Term Evolution) or IMT-Advanced (International Mobile Telecommunications) [1], which promises to encompass two main legacy technologies among others, namely cellular and WLAN (id., IEEE 802.xx). 4G promises to deliver high-speed wireless data transmission services at much lower costs and latencies while providing much higher rates, spectrum efficiencies and coverage. Most importantly, it promises the provision of future high-speed wireless data services everywhere closer to the mobile user in a seamless and versatile fashion, no matter what the surrounding environment and link conditions are. This stringent requirement calls for the development of new cognitive transceivers that are capable of promptly and properly self-adapting to variable operating conditions in order to constantly maximize their performance.

It is precisely in this vibrant research context that we get

onto the emerging cognitive radio [2], [3] from a rather uncommon perspective today. Indeed, cognitive radio is reduced in most recent works to one of its two primary objectives: exploit efficiently the radio spectrum with dynamic spectrum access (DSA) that allocates the least occupied frequencies, though licensed and reserved, to secondary users who are short of bandwidth [4]- [6]. Here we take up its second primary objective of providing highly reliable communications anywhere anytime, so far addressed in a conventional manner, but rarely tackled today from a new level of "cognitive wireless communications" [3] where cognition could possibly handle many dynamic reconfiguration dimensions other than spectrum allocation, the conventional one. Explicitly, we aim at developing a new context-aware cognitive transceiver (CTR) which is able to self-adjust its antenna-array processing structure and air-interface configuration for optimum performance. Cognition ability of our new context-aware CTR amounts to selecting the best combination triplet of pilot-use, channel-identification, and data-detection modes that achieve the best link-level throughput performance against channel conditions in terms of channel type, mobile speed, SNR, and CQI.

II. CONTEXT-AWARE COGNITIVE TRANSCEIVER MODES

A. DA or pilot-assisted mode

Pilot symbols are reference (i.e., known) symbols inserted according to a predefined mapping to be used by the receiver for channel estimation and synchronization purposes. The LTE downlink pilot mapping is described in Fig. 1.

1) LS channel estimator: This conventional estimator uses pilot symbols to estimate the channel by minimizing the squared difference between the received signal and the known pilot symbols. Let $y_{i,\text{DA}}$ denote the received signal on pilot sub-carrier i among N_{pilot} pilot sub-carriers at the OFDM pilot symbol index t. For convenience, we will henceforth omit the time index t. The transmitted pilot symbol $x_{i,\text{DA}}$ is related to $y_{i,\text{DA}}$ as follows:

$$y_{i,\text{DA}} = h_i x_{i,\text{DA}} + n_i \qquad i = 0, 1, ..., N_{pilot} - 1 \quad (1)$$

where h_i is the complex channel coefficient and n_i is a zero-mean Gaussian noise. The matrix notation of (1) is given by:

$$\mathbf{y}_{\text{DA}} = \mathbf{X}_{\text{DA}}\mathbf{h} + \mathbf{n} \quad (2)$$

where $\mathbf{X}_{\text{DA}} = \text{diag}\left\{x_{0,\text{DA}}, x_{1,\text{DA}}, \ldots, x_{N_{pilot}-1,\text{DA}}\right\}$, $\mathbf{h} = [h_0, h_1, ..., h_{N_{pilot}-1}]^T$, and $\mathbf{n} = [n_0, n_1, ..., n_{N_{pilot}-1}]^T$ is the i.i.d complex zero-mean Gaussian noise vector. The LS algorithm aims at minimizing $(\mathbf{y}_{DA} - \mathbf{X}_{DA}\mathbf{h})^\dagger (\mathbf{y}_{\text{DA}} - \mathbf{X}_{\text{DA}}\mathbf{h})$ († denotes matrix Hermitian transpose) to estimate the channel frequency response thereby leading to [7]:

$$\widehat{\mathbf{h}}_{\text{LS}} = \mathbf{X}_{\text{DA}}^{-1}\mathbf{y}_{\text{DA}}, \quad (3)$$

Fig. 1. LTE downlink pilot mapping.

Fig. 2. LTE downlink pilot mapping used for NDA with pilot RLS channel identification.
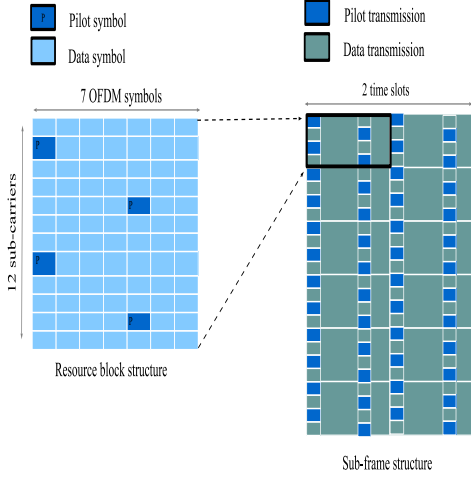
where $\mathbf{A}^{-1}$ denotes the matrix inverse. The estimates for the channel coefficients at non-pilot subcarriers can then be easily obtained by interpolation [10]. However, when the channel is fast fading (i.e., high user velocity), the pilot symbols spacing may not be sufficient to enable proper tracking of the channel variations. Moreover, increasing pilot overhead leads to a throughput decrease which is not desirable for any communication system.

2) ML estimator: Here, we consider the ML channel estimator developed in [8]. For each OFDM symbol, the DA ML estimator captures the channel's time variations via a polynomial-in-time expansion of order $(J-1)$. In fact, the channel over each $\{r^{th}\}_{r=1}^{N_r}$ antenna branch and the ith subcarrier, in a SIMO system, is modeled as follows [9]:

$$h_{i,r}(t_n) = \sum_{j=0}^{J-1} c_{i,r}^{(j)} t_n^j + REM_J^{(i,r)}(t_n). \quad (4)$$

Here, $t_n = nT_s$ with T_s being the sampling period. The polynomial order $J-1$ is a Doppler-dependent parameter optimized in [8]. Moreover, $c_{i,r}^{(j)}$ is the jth coefficient of the channel polynomial approximation over the ith sub-carrier and the rth branch. As will be explained shortly, the term $REM_J^{(i,r)}(t_n)$ refers to the remainder of the Taylor series expansion which can be driven to zero by choosing an approximation window of sufficiently small size thereby yielding the following accurate approximation [8]:

$$h_{i,r}(t_n) = \sum_{j=0}^{J-1} c_{i,r}^{(j)} t_n^j. \quad (5)$$

Channel estimation is performed independently over each pilot sub-carrier. For the sake of simplicity, we also omit the sub-carrier index in the remainder of this paper.
To use a small model order $J-1$ in (4) and thereby avoid costly inversions of large-size matrices, the new DA ML estimator partitions the whole observation window into K local approximation windows of the same size. Then, it maximizes the probability density function (pdf) of the locally-observed vectors, $\mathbf{y}_{\mathrm{DA}}^{(k)}$, parametrized by $\mathbf{c}_k$:

$$p(\mathbf{y}_{\mathrm{DA}}^{(k)}; \mathbf{c}_k | \mathbf{B}_k)$$
$$= \frac{1}{(2\pi\sigma^2)^{N_{\mathrm{DA}}N_r}} \exp\left\{-\frac{1}{2\sigma^2}\left[\mathbf{y}_{\mathrm{DA}}^{(k)} - \mathbf{B}_k\mathbf{c}_k\right]^H\left[\mathbf{y}_{\mathrm{DA}}^{(k)} - \mathbf{B}_k\mathbf{c}_k\right]\right\}, \quad (6)$$
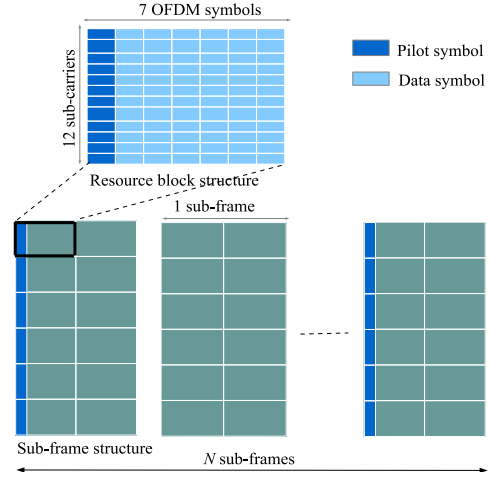
where $\mathbf{c}_k$ is a vector containing the unknown approximation polynomial coefficients over the kth approximation window (i.e., for all the antenna branches) defined as $\mathbf{c}_k = [\mathbf{c}_{k,1}^T, \mathbf{c}_{k,2}^T, ..., \mathbf{c}_{k,N_r}^T]^T$ with $\mathbf{c}_{k,r} = [c_{k,r}^{(0)}, c_{k,r}^{(1)}, ..., c_{k,r}^{(J-1)}]^T$ where $c_{k,r}^{(j)}$ is the jth coefficient of the channel polynomial approximation over the ith sub-carrier, the kth approximation window and the rth branch and σ^2 defines the noise variance. In (6), $\mathbf{y}_{\mathrm{DA}}^{(k)} = [\mathbf{y}_{1,\mathrm{DA}}^{(k)} \mathbf{y}_{2,\mathrm{DA}}^{(k)} \cdots \mathbf{y}_{N_r,\mathrm{DA}}^{(k)}]^T$ with $\mathbf{y}_{r,\mathrm{DA}}^{(k)}$ being the received pilot samples over the antenna element r within the kth approximation window, i.e., $\mathbf{y}_{r,\mathrm{DA}}^{(k)} = [y_r^{(k)}(t_1) y_r^{(k)}(t_2) ... y_r^{(k)}(t_{P_{\mathrm{DA}}})]$. Here P_{DA} is the number of pilot symbols in each approximation window which is covering N_{DA} pilot and non-pilot received samples. The approximation window size N_{DA} is another Doppler-dependent design parameter optimized in [8]. Moreover $\mathbf{B}_k$ is a $P_{\mathrm{DA}}N_r \times JN_r$ block-diagonal matrix defined as $\mathbf{B}_k =$ blkdiag$\{\mathbf{A}_k\mathbf{T}, \mathbf{A}_k\mathbf{T}, ..., \mathbf{A}_k\mathbf{T}\}$. Here, $\mathbf{A}_k$ is the $P_{\mathrm{DA}} \times P_{\mathrm{DA}}$ diagonal matrix of the transmitted pilot symbols within the kth observation window, i.e., $\mathbf{A}_k = \mathrm{diag}\{a_k(t_1), a_k(t_2), ..., a_k(t_{P_{\mathrm{DA}}})\}$, and $\mathbf{T}$ is a Vandermonde matrix given by:

$$\mathbf{T} = \begin{pmatrix} 1 & t_1 & ... & t_1^{J-1} \\ 1 & t_2 & ... & t_2^{J-1} \\ \vdots & \vdots & \ddots & \vdots \\ 1 & t_{P_{DA}} & ... & t_{P_{DA}}^{J-1} \end{pmatrix}. \quad (7)$$

The estimate of the channel coefficients over all the receiving antenna branches are obtained by setting the partial derivative of (6) [or its natural logarithm] to zero yielding:

$$\widehat{\mathbf{c}}_{k,\mathrm{DA}} = (\mathbf{B}_k^\dagger \mathbf{B}_k)^{-1} \mathbf{B}_k^\dagger \mathbf{y}_{\mathrm{DA}}^{(k)}, \quad (8)$$

from which the DA ML estimates for the channel coefficients at both pilot and non-pilot positions are obtained by injecting the estimates of the polynomial coefficients established in (8) back into (4).

B. NDA with pilot or hybrid mode

Ensuring reliable communications is the purpose of all wireless communication systems. However, receiver mobility and surrounding scatterers' motion make channel estimation

Number of User Equipment	1
Channel Bandwidth (MHZ)	1.4
Carrrier Frequency (GHZ)	2.1
Frame Duration (ms)	10
subframe Duration (ms)	1
Sub-carrier Spacing (kHz)	15
FFT size	128
Number of Resource Blocks	6
Number of subcarriers/RB	12
DL Bandwidth Efficiency	77.1%
OFDM Symbols/subframe	7
CP length (μs)	5.2 (first symbols)/4.69 (six following symbols)
Transmit mode	SIMO
Channel type	PedA, VehA, and VehB
channel coding	convolutional turbo encoder

TABLE II.   MULTIPATH POWER DELAY PROFILE OF PEDA, VEHA, AND VEHB CHANNELS.

Channel type	Relative Delay (ns)	Relative power (dB)
PedA	0	0
	110	-9.7
	190	-19.2
	410	-22.8
VehA	0	0
	310	-1
	710	-9
	1090	-10
	1730	-15
	2510	-20
VehB	0	-2.5
	300	0
	8900	-12.8
	12900	-10
	17100	-25.2
	20000	-16

accuracy a truly challenging task. For that reason, pilot symbols that are inserted far apart, in the time-frequency grid, do not enable accurate tracking of fast-varying channels. Information carried in data symbols is hereafter exploited in a hybrid channel identification scheme in order to enhance the system performance.

1) NDA w. pilot RLS estimator: At OFDM symbol $t + 1$, we use preceding transmitted signals as a training sequence of t symbols. In fact, the channel estimate, $\widehat{\mathbf{H}}_{t+1}$, at OFDM symbol $t + 1$ is obtained using the weighted LS method as follows [11]:

$$\widehat{\mathbf{H}}_{t+1} = \arg\min_{\widehat{\mathbf{H}}} \sum_{w=1}^{t} \beta_w \|\mathbf{y}_w - \widehat{\mathbf{H}}\mathbf{Q}_w x_w\|^2, \qquad (9)$$

where the channel variation $\mathcal{H}$ is approximated to the Dth order Taylor series expansion according to the OFDM symbol instance m, i.e.: $\mathcal{H}_w \simeq \sum_{d=0}^{D} w^d \mathcal{H}^{<d>} = \mathbf{H}\mathbf{Q}_w$ with $\mathbf{Q}_w \triangleq [w^0\mathbf{I}_{N_r}, w^1\mathbf{I}_{N_r}, ..., w^D\mathbf{I}_{N_r}]^T \in \mathbb{R}^{N_r(D+1)\times N_r}$. In (9) $\beta_w \in \mathbb{R}$ stands for a weighting coefficient given by $\beta_w = \lambda^{t-w}$ where $\lambda \in \mathbb{R}$ is referred to as a forgetting factor. The exponential weighted RLS algorithm is implemented as follows:

$$\boldsymbol{\zeta}_t = \boldsymbol{\Phi}_{t-1}^{-1}\mathbf{Q}_t x_t \in \mathbb{C}^{N_r(D+1)\times 1},$$
$$\alpha_t = \frac{1}{\lambda + \boldsymbol{\zeta}_t^{\dagger}\mathbf{Q}_t x_t} \in \mathbb{R},$$
$$\boldsymbol{\Phi}_t^{-1} = \lambda^{-1}\boldsymbol{\Phi}_{t-1}^{-1} - \lambda^{-1}\alpha_t\boldsymbol{\zeta}_t\boldsymbol{\zeta}_t^{\dagger} \in \mathbb{C}^{N_r(D+1)\times N_r(D+1)},$$
$$e_t = y_t - \widehat{\mathbf{H}}x_t \in \mathbb{C}$$
$$\widehat{\mathbf{H}}_{t+1} = \widehat{\mathbf{H}}_t + \alpha_t e_t \boldsymbol{\zeta}_t^{\dagger} \in \mathbb{C}^{1\times N_r(D+1)}.$$

For initialization, $\widehat{\mathbf{H}}_1$ is considered to be identically zero and $\boldsymbol{\Phi}_0^{-1}$ is set to $\varrho\mathbf{I}_{N_r(D+1)}$ where $\varrho \gg 1$ is a constant with sufficiently large value. Moreover, x_1 is assumed to be a pilot symbol. The channel estimate $\widehat{\mathbf{H}}_{t+1}$ is then used to detect the $(t+1)^{th}$ symbol x_{t+1}. The pilot mapping used for the RLS channel estimator is described in Fig. 2. We note that the pilot symbols insertion frequency is optimized by simulations depending on the mobile speed. For mobile speed=2 kmph, 30 kmph and 100 kmph, respectively, pilot symbols are inserted each 10, 2 and 1 subframes. These values are expected because as the channel variations get fast, we need more pilots to truck the channel.

2) NDA w. pilot ML estimator: We consider the expectation maximization (EM) based ML estimator developed in [8]. The new estimator uses pilot and data symbols jointly in order to track the channel variations. The pilot mapping used

for the "NDA with pilot" ML estimator is described in Fig. 1. In a first step and for a given sub-carrier, the NDA with pilot estimator relies on pilot symbols to estimate the channel coefficients at pilot OFDM symbols as described in Section II-A2. In a second step, the NDA with pilot estimator applies the EM algorithm over all the received samples in order to jointly estimate the channel coefficients and detect the transmitted unknown symbols at non-pilot positions as well. The iterative EM algorithm runs in two main steps and uses as initialization $\widehat{\mathbf{c}}_{k,\text{DA}}$ obtained in (8) from pilot positions only.

● Expectation step (E-Step):

During the E-Step, the pdf function defined in (6) takes into account all the possible transmitted symbols $\{a_m\}_{m=1}^{M}$ where M is the modulation order. In fact, at each iteration q, for every approximation window of size N_{NDA} symbols, the objective function is updated as follows:

$$Q(\mathbf{c}_k \mid \widehat{\mathbf{c}}_k^{(q-1)}) = -N_{\text{NDA}}N_r \ln(2\pi\sigma^2)$$
$$-\frac{1}{2\sigma^2}\sum_{r=1}^{N_r}\left(M_{2,k}^{(r)} + \sum_{n=1}^{N_{\text{NDA}}}\alpha_{n,k}^{(q-1)}|\mathbf{c}_{r,k}^T\mathbf{t}(n)|^2 - 2\beta_{r,n,k}^{(q-1)}\mathbf{c}_{r,k}\right), \quad (10)$$

where $M_{2,k}^{(r)} = E\{|y_{r,k}(n)|^2\}$ is the second-order moment of the received samples over the rth receiving antenna branch, $\mathbf{t}(n) = [1, t_n, t_n^2, ..., t_n^{J-1}]^T$ and:

$$\alpha_{n,k}^{(q-1)} = \sum_{m=1}^{M} P_{m,n,k}^{(q-1)}|a_m|^2, \qquad (11)$$

$$\beta_{r,n,k}^{(q-1)}(\mathbf{c}_{r,k}) = \sum_{m=1}^{M} P_{m,n,k}^{(q-1)}\Re\{y_{r,k}^*(n)a_m\mathbf{t}^T(n)\mathbf{c}_{i,k}\}. \quad (12)$$

Here, $P_{m,n,k}^{(q-1)} = P(a_m \mid \mathbf{y}_k(n); \widehat{\mathbf{c}}^{(q-1)})$ is the *a posteriori* probability of a_m at iteration $(q-1)$ that is computed using the Bayes' formula as follows:

$$P_{m,n,k}^{(q-1)} = \frac{P(a_m)P(\mathbf{y}_k(n)|a_m; \widehat{\mathbf{c}}_k^{(q-1)})}{P(\mathbf{y}_k(n); \widehat{\mathbf{c}}_k^{(q-1)})}. \qquad (13)$$

Since the symbols are assumed to be equally likely transmitted, we have $P(a_m) = \frac{1}{M}$ and therefore:

$$P(\mathbf{y}_k(n); \widehat{\mathbf{c}}_k^{(q-1)}) = \frac{1}{M}\sum_{m=1}^{M} P(\mathbf{y}_k(n)|a_m; \widehat{\mathbf{c}}_k^{(q-1)}). \qquad (14)$$
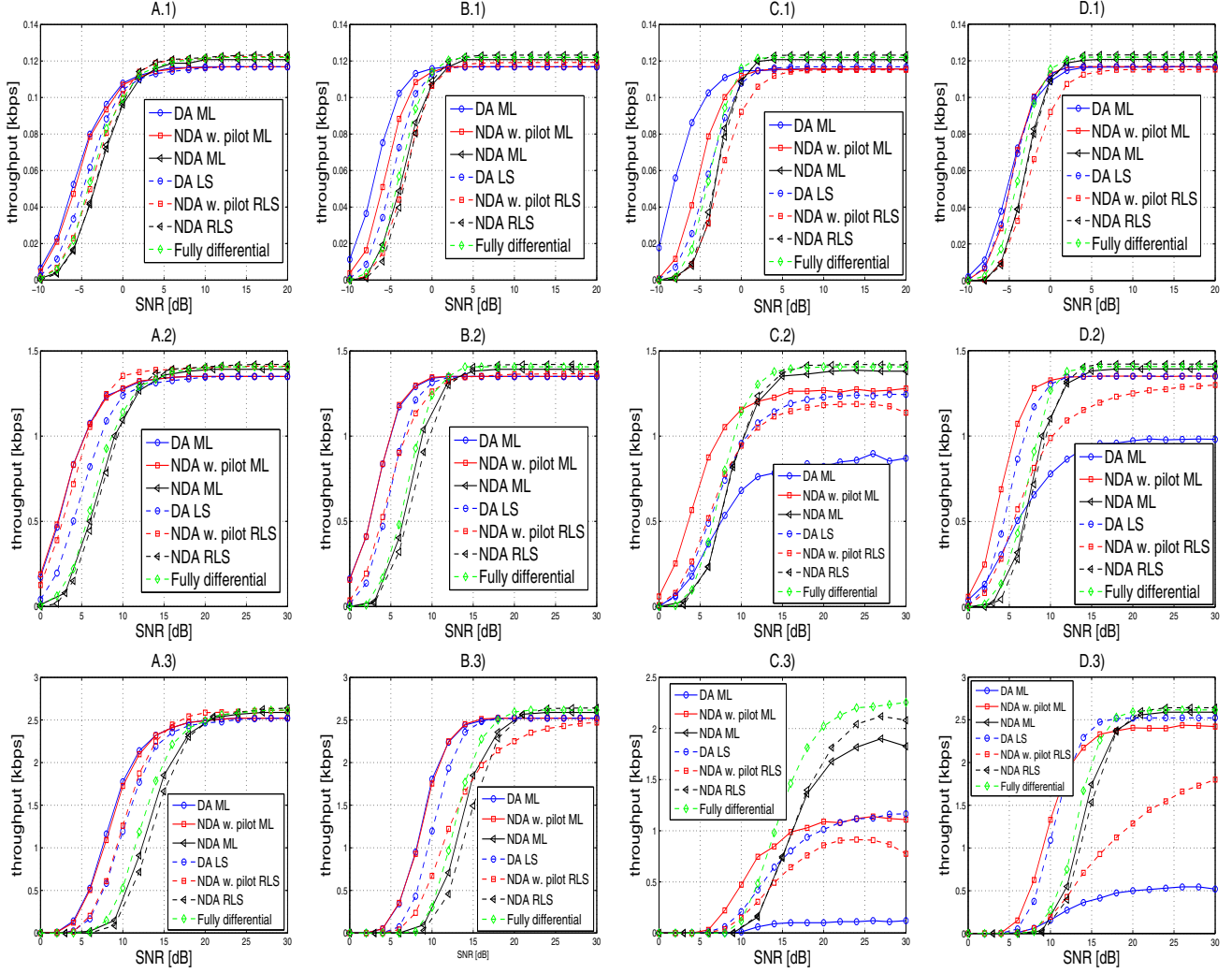
Fig. 3. LTE downlink link-level throughput performance for A) PedA channel/speed=2 km/h, B) VehA channel/speed=30km/h, C) VehB channel/speed=100 km/h, and D) VehA channel/speed=100 km/h; and 1) CQI=1 for QPSK, 2) CQI=7 for 16QAM, and 3) CQI=10 for 64QAM.

• Maximization step (M-Step):

During the M-Step, the objective function obtained in (10) is maximized with respect to $\mathbf{c}_k$:

$$\widehat{\mathbf{c}}_k^{(q)} = \underset{\mathbf{c}_k}{\arg\max}\, Q\big(\mathbf{c}_k|\widehat{\mathbf{c}}_k^{(q-1)}\big), \tag{15}$$

yielding the following more refined estimates for the approximation polynomial coefficients, i.e.:

$$\widehat{\mathbf{c}}_{r,k}^{(q)} = \left(\sum_{n=1}^{N_{\text{NDA}}} \mathbf{t}(n)\mathbf{t}^T(n)\right)^{-1} \sum_{n=1}^{N_{\text{NDA}}} \lambda_{r,n,k}^{(q-1)}\mathbf{t}(n). \tag{16}$$

In (16), $\lambda_{r,n,k}^{(q-1)}$ is given by:

$$\lambda_{r,n,k}^{(q-1)} = \left[\widehat{a}_k^{(q-1)}(t_n)\right]^* y_{r,k}(t_n), \tag{17}$$

in which

$$\widehat{a}_k^{(q-1)}(t_n) = \sum_{m=1}^{M} P_{m,n,k}^{(q-1)} a_m, \tag{18}$$

is the soft symbol estimate at iteration $q-1$ and $\mathbf{t}(n) = [1, t_n, t_n^2, ..., t_n^{J-1}]^T$.

C. NDA or blind mode

For blind or NDA channel estimation, no pilot symbols are exploited by the receiver. Channel estimation is performed based on the information carried by all symbols assumed unknown a priori. Phase ambiguity is resolved by differential modulation. The blind RLS channel estimator algorithm is already the one described in Section II-B1. However, an arbitrary guess of the first sent symbol is used to initialize the recursive algorithm. The blind channel estimation algorithm is also the one described in Section II-B2. The only difference here, however, is that the initialization is arbitrary and random.

D. Data detection modes

On the top of selecting the appropriate channel estimator and pilot-use couples among DA ML, NDA w. pilot ML, NDA ML, DA LS, NDA w. pilot RLS and NDA RLS, the new context-aware CTR selects one of the following data detection modes:
• Coherent if pilot symbols are used.
• Non coherent or differential if no pilot symbols are used.
We also implement a "fully differential" transceiver version for which no channel estimation is required. Data detection is
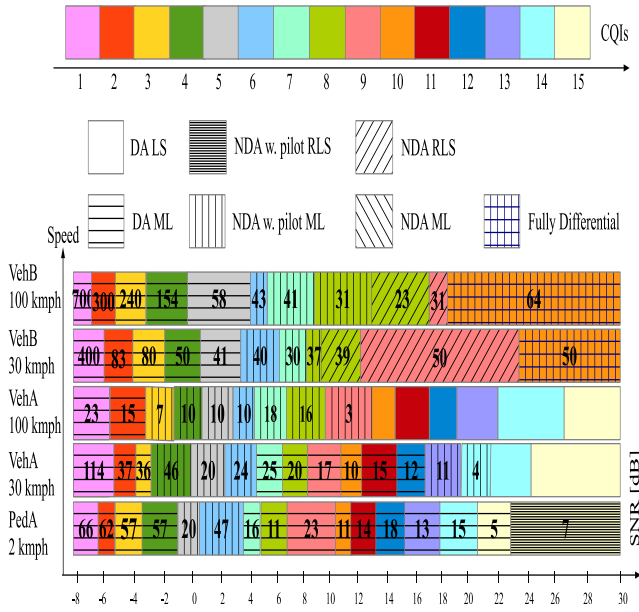
Fig. 4. Decision rules of the cognitive transceiver and throughput gain percentages against the conventional DA LS estimator with coherent detection versus SNR for different channel types and mobile speeds.

only based on differential modulation-demodulation. We use the soft-decision-aided DAPSK detection algorithm developed in [12] and [13].

III. SIMULATION SETUP AND RESULTS

A 1×2 antenna configuration (1 transmit antenna at the eNodeB and 2 receive antennas at the mobile) is adopted as a SIMO configuration example for discussion in the rest of the paper. Some of the LTE downlink link-level parameters are summurized in Table I. Our main goal is to select 1) the best channel identification mode that yields the highest link-level throughput among DA, NDA w. pilot (i.e., hybrid) and completely NDA; 2) the best detection mode between coherent and differential; both against the operating conditions in terms of SNR, channel model type, mobile speed, and CQI value. In this paper, we consider a Pedestrian A (PedA) flat-fading channel for a mobile speed of 2 km/h and a Vehicular A and B (VehA and VehB) frequency-selective channels for mobile speeds of 30 km/h and 100 km/h. PedA and VehA channel's power delay profiles (PDPs) are given in Table II. The CQI value indicates to the eNodeB the modulation order and the channel coding rate to be used during each subframe. The CQI values range from 1 to 15 defining six, three, and six coding rates for QPSK/DPQSK, 16QAM/D16Star-QAM, and 64QAM/D64Star-QAM modulations, respectively. In our simulations, the SNR and CQI values are assumed to be known by the receiver. Due to lack of space, we only show throughput results of CQI 1 (QPSK), CQI 7 (16QAM) and CQI 10 (64QAM). As shown in Figs. 3.A) and 4, the DA ML outperforms the DA LS estimator by over 50% throughput gain in the low SNR region over the PedA channel. This is because modeling the channel with Taylor series remains accurate when the channel experiencs flat fading. In Figs. 3.B) and 4 for a medium mobile speed, NDA w. pilot offers throughput gains between 40% and 20%. This is due to the fact that relying on data symbols jointly with pilot symbols enhances channel estimation when time variations are significant. Figs. 3.D) and

4 confirm this fact since the SNR range over which NDA w. pilot ML offers remarkable throughput gains increases at higher velocity over the VehA channel and a mobile speed of 100 km/h. For the VehB channel and a mobile speed of 100 km/h, Figs 3.C.1) and 4 reveal a gain as high as 700% that is offered by DA ML as compared to DA LS in terms of link-level throughput, in the low SNR region. For the same channel type and mobile speed, Figs 3.C) and 4 suggest that NDA RLS and the fully-differential version offer throughput gains rising up to 60% in the high SNR region for CQIs 8, 9 and 10. This can be explained by the fact that the use of pilot symbols is no longer reliable with high-order modulations due to their extreme sensitivity to channel estimation errors.

IV. CONCLUSION

In this paper, we were able to emphasize the link-level throughput gains achievable by a new context-aware cognitive SIMO transceiver (CTR) able to select the pilot-use mode for channel identification between conventional DA, new NDA w. pilot, and NDA; the best channel estimator between LS and ML; and the best detection mode between coherent and differential; all against channel conditions in terms of channel speed, channel type, SNR, and CQI. The throughput gains achievable by the new context-aware CTR are noticeable in most operating conditions. Moreover they increase significantly with adversity at relatively lower SNR values, higher mobile speeds, and larger channel selectivity to reach as much as 700%.

REFERENCES

[1] F. Khan, *LTE-Advanced for 4G Mobile broadband air interface technologies and performance*, Cambridge University Press, 2009.

[2] J. Mitola III, *Cognitive radio architecture*, John Wiley & Sons, 2006.

[3] S. Haykin, "*Cognitive radio: brain-empowered wireless communications*", *IEEE JSAC.*, vol. 3, no. 2, pp. 201-220, Feb. 2005.

[4] W. Krenik, A.M. Wyglinski, and L.E. Doyle, "Cognitive radios for dynamic spectrum access", *IEEE TCOM.*, vol. 45, no. 5, pp. 64-65, May 2007.

[5] J.W. Huang and V. Krishnamurthy, "Cognitive base stations in LTE/3GPP femtocells: a correlated equilibrium game-theoretic approach," *IEEE TCOM.*, vol. 59, no. 12, pp. 3485-3493, Dec. 2011.

[6] A. Attar, V. Krishnamurthy, and O.N. Gharehshiran, "Interference management using cognitive base-stations for UMTS LTE," *IEEE Commun. Mag.*, vol. 49, no. 8, pp. 152-159, Aug. 2011.

[7] J.-J. Van de Beek *et al* "On channel estimation in OFDM systems," in *Proc. IEEE 45th VTC.*, 1995, vol. 2, pp. 815-819.

[8] F. Bellili, R. Meftehi, S. Affes, and A. Stéphenne, "Maximum likelihood SNR estimation of einearly-modulated signals over time-varying flat-fading SIMO channels," *IEEE TSP.*, vol. 63, no. 2, pp. 441-456. Jan. 2015.

[9] P. Bello, "Characterization of randomly time-variant linear channels," *IEEE TCOM.*, vol. 11, no. 4, pp. 360-393, Dec. 1963.

[10] S. Omar , A. Ancora, and D.T.M. Slock, "Performance analysis of general pilot-aided linear channel estimation in LTE OFDMA systems with application to simplified MMSE schemes," in *Proc IEEE 19th PIMRC*, 2008.

[11] T.K. Akino, "Optimum weighted RLS channel estimation for rapid fading mimo channels," *IEEE TWireless.*, vol. 7, no. 11, pp. 4248-4260, Nov. 2008.

[12] D. D. Liang, S. X. Ng. Soon, and L. Hanzo, "Soft-decision star-QAM aided BICM-ID," *IEEE SPL.*, vol. 18, no. 3, pp. 169-172, Mar. 2011.

[13] C. Xu, D. Liang, S. X. Ng, and L. Hanzo, "Reduced-complexity noncoherent soft-decision-aided DAPSK dispensing with channel estimation," *IEEE TVT.*, vol. 62, no. 6, pp. 2633- 2643, July 2013.